

# Hidden Breakthroughs in Language Model Training

Sara Kangaslahti  
Harvard University  
sarakangaslahti@harvard.edu

Elan Rosenfeld  
Google Research  
elanr@google.com

Naomi Saphra  
Harvard University  
nsaphra@fas.harvard.edu

## Abstract

Loss curves are smooth during most of model training, so visible discontinuities stand out as possible conceptual breakthroughs. Studying these breakthroughs enables a deeper understanding of learning dynamics, but only when they are properly identified. This paper argues that similar breakthroughs occur frequently *throughout* training but they are obscured by a loss metric that collapses all variation into a single scalar. To find these hidden transitions, we introduce POLCA, a method for decomposing changes in loss along arbitrary bases of the low-rank training subspace. We use our method to identify clusters of samples that share similar changes in loss during training, disaggregating the overall loss into that of smaller groups of conceptually similar data. We validate our method on synthetic arithmetic and natural language tasks, showing that POLCA recovers clusters that represent interpretable breakthroughs in the model’s capabilities. We demonstrate the promise of these hidden phase transitions as a tool for unsupervised interpretability.

## 1 Introduction

As large language models train, various internal structures develop during abrupt phase transitions. These sudden drops in loss reveal the formation of mechanisms for in-context learning [25], natural language grammar [6], hierarchical generalization [21], and many other concepts [19, 16, 27, 1]. However, the loss curve as a whole remains stubbornly smooth. As a result, these momentary conceptual breakthroughs are treated as isolated curiosities, while the majority of training behavior is considered predictable.

This work shows that in fact, a model undergoes many breakthroughs during training, most which are concealed when averaging all data into a single loss curve. Instead, we divide up the loss curve in two different ways to find hidden breakthroughs. First, we **disaggregate** the **aggregate** loss into losses on individual examples. By clustering the individual loss curves, we identify subsets of data that experience synchronized changes in loss, implying that they rely on the same conceptual breakthrough. However, any individual example might benefit from *multiple* breakthroughs; such an example may undergo changes synchronized with different data subsets at different times. Furthermore, distinct concepts might appear simultaneously, erroneously merging their data clusters. This means we may have to identify multiple separate breakthroughs which affect the loss curve of a single example.

To disentangle these effects for a single sample, we separate the optimization space into specific gradient directions. When the loss changes during training, it is the result of movement across all parameters in a high-dimensional space. We **decompose** this loss change from an **exact** trajectory in the full-rank parameter space into a collection of movements along each dimension. By analyzing these loss curves along specific basis vectors, we identify conceptual breakthroughs that rely on particular directions of movement. The latter analysis permits further granularity in clustering data, as final performance on an individual example may rely on multiple conceptual breakthroughs, each corresponding to a particular linear direction in training. In summary:

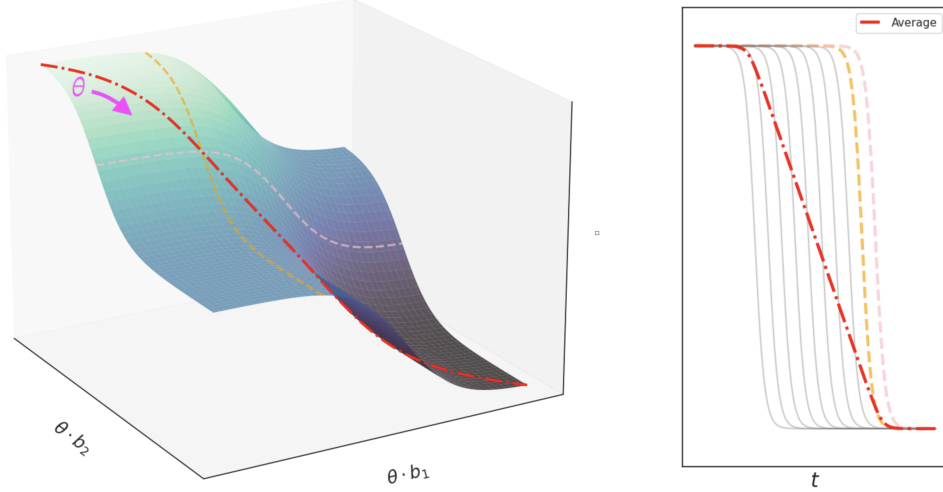


Figure 1: A smooth loss function may change sharply for a particular direction or data subset. POLCA works by decomposing and disaggregating the loss to discover these sharp changes. *Left:* Loss  $L(x; \theta)$  changes as the parameter setting  $\theta$  moves in a low-rank training subspace. The loss is sigmoidal on each axis, with differently timed inflections along basis vectors  $b_1$  and  $b_2$ . These breakthroughs disappear in the smooth **sum** of the sigmoids which represents the exact loss. *Right:* The **average** of sigmoidal functions—including loss along basis vectors  $b_1$  and  $b_2$ —elides individual breakthroughs. The more differently-timed breakthroughs underlie the loss, the more hidden each breakthrough is.

- We introduce a modified form of Loss Change Allocation [15] called **Projection Oriented Loss Change Allocation (POLCA)** to measure changes in loss due to parameter adjustments in arbitrary directions during training (Section 3.2).
- We show that some learned concepts can be identified by clustering exact loss, while others cannot (Section 4.2).
- Using POLCA, we extend our cluster analysis to identify conceptual breakthroughs in a restricted gradient subspace that are obscured in the exact loss curves. We automatically identify specific concepts learned during breakthroughs in both synthetic (Section 4) and natural language settings (Section 5).

## 2 Background: How much can we learn from learning dynamics?

Various loss phase transitions have been interpreted as conceptual breakthroughs. But why expect additional interpretable breakthroughs to underlie periods of undifferentiated, gradual model improvement? Our approach is justified by the nature of the loss surface’s complexity, illustrated by Figure 1, in which a smooth curve emerges by eliding phase transitions from each dimension.

**Why expect multiple phase transitions?** A very early phase transition is to be expected early in training after a brief memorization stage [30]. In this sense, the most celebrated breakthroughs are not the first phase transitions in their training curves. Some breakthroughs even depend on earlier breakthroughs, as observed in synthetic tasks [1] and in grammar acquisition [6]. If one concept depends on another, each must appear at a different timestep, requiring multiple phase transitions.

Multiple phase transitions can also come from differences in gradient scale along different directions. Ma et al. [18] even attributed the early edge-of-stability phase transition [13, 8] to multiscale structure of the loss surface and, furthermore, noted that this multiscale structure emerges at the range where models become *singular*: their loss lacks a quadratic approximation in terms of model parameters, creating conditions for phase transitions under Singular Learning Theory [33, 34, 32]. They argued that this structure is the product of both *nonuniform data* and *nonconvex objectives*, respectively justifying the *disaggregation* and *decomposition* which we apply to interpret training dynamics.

**Why disaggregate the aggregate loss?** We track learning on training datapoints and subpopulations, rather than the whole training set, because relevant skills can be acquired at different rates [3, 7]. Individual samples thus exhibit changes in loss out of line with the monotonic average trend [36, 29]. In full-batch gradient descent, Cohen et al. [8] identified non-monotonicity arising from oscillation about the maximum Hessian eigenvector. Rosenfeld and Risteski [29] demonstrated that these oscillations occur across different axes for different samples and identified the primary cause: surprisingly human-interpretable semantic features. Even when the loss seems stable, performance can oscillate on edge cases until the model develops relevant capabilities [28, 4]. We hypothesize that oscillation represents competing skills that are relevant to different subsets of data. To test this hypothesis, and to interpret the meaning of these directions, we disaggregate the loss into clusters with similar dynamics.

**Why decompose the exact loss?** Our POLCA decomposition addresses what Michaud et al. [20] called *polygenic* scaling effects—samples which combine multiple skills and therefore exhibit breakthroughs at multiple scales. If we assume that a specific skill is enabled by movement along a particular skill’s basis vector, then the loss change attributed to movement along that vector will accelerate at the moment the skill is acquired, for every sample that requires that skill. In this manner, the sample transitions from early to late dynamics through a basis-specific loss phase transition. In other words, by monitoring changes in directions corresponding to specific skills, we support the speculation of Nanda et al. [23] that “*phase transitions are everywhere.*”

**Why is linear decomposition sufficient?** In practice, a conceptual breakthrough might not occur in a single direction that persists throughout training. However, there is an abundance of evidence that linear bases of the low-rank [12] training subspace are conceptually meaningful. In the late stages of training, loss is convex on the line connecting a pair of checkpoints [10] if those checkpoints express similar capabilities [14] and mechanisms [17]. If a pair of high-dimensional models lack this linear connection, they still connect nonlinearly [9]; however, while parameter settings sampled from their linear connections improve broadly on the capabilities of the original models, those sampled from their nonlinear connections are less robust than the originals [14, ref Appendix D]. These observations suggest that linear decomposition should preserve meaningful conceptual features on the loss surface, and our experiments show that the resulting directions are interpretable in practice.

### 3 Methods

The key to our approach is the separate consideration of how each example’s **datapoint loss** changes throughout training. We contrast this individualized metric with **aggregated loss** across an entire dataset. Using the datapoint loss, we can cluster individual examples on the basis of their loss  $L(w_t)$ , change in loss  $L(w_t) - L(w_{t-1})$ , or magnitude of change  $|L(w_t) - L(w_{t-1})|$  during training.

Our objective is to decompose the loss itself into specific directions in the weight space, motivated by several considerations: First, while we have moved from an aggregated loss metric to a more granular datapoint loss metric, we are still only considering breakthroughs that are general enough to be perceived in loss curves. Second, an individual datapoint may benefit from a variety of conceptual breakthroughs, but will not be clustered on the breakthroughs individually. Finally, once we have identified a subset of the data as benefiting from a particular conceptual breakthrough, decomposing into individual weight directions allows us to locate where in the weights the breakthrough occurs and to thereby identify the mechanism involved.

Next we break this loss down by directional movement during training, allowing us to discover breakthroughs that are specific to a given direction. Our procedure follows three steps: (1) select a basis, (2) decompose the loss along that basis to highlight particular learning events, (3) cluster datapoints according to their shared learning events.

#### 3.1 Finding the basis

To decompose the loss, we first require an interpretable orthogonal basis. We efficiently compute the eigenvectors of the Hessian matrix with CoLA [26] and use them to construct a restricted training subspace. We posit this basis to be interpretable because each basis vector expresses a high gradient

---

**Algorithm 1** Finding the decomposed optimization basis

---

**input:** Training set  $X$ , Model checkpoints  $\{\theta_t\}_{t=1}^T$ .  
 $B \leftarrow \emptyset \in \mathbb{R}^{d \times 0}$ .  
**for**  $t = 1 \dots T$  **do**  
     $\Pi_{\perp} \leftarrow I - B(B^{\top} B)^{-1} B^{\top}$   
     $\mathcal{H} \leftarrow \nabla_{\theta}^2 \mathcal{L}(X, \theta)$ .  
    Define  $B^+ \in \mathbb{R}^{d \times k}$  as the top  $k$  eigenvectors of  $\Pi_{\perp} \mathcal{H}$  (e.g., via the Lanczos method).  
     $B \leftarrow [B, B^+]$ .  
**end for**  
**return**  $B$

---

covariance and therefore represents a potential decision boundary. While we select this basis for interpretability, our approach can use any arbitrary choice of basis.

This basis is constructed as shown in Algorithm 1. Given  $T$  intermediate training checkpoints and a number  $k$  of eigenvectors to compute at each checkpoint, we seek a low rank  $Tk$ -dimensional subspace which captures most of the movement during optimization [12]. We construct this basis iteratively, starting with  $B = \emptyset$ : at each checkpoint  $t$ , we take checkpoint weights  $W_t \in \mathbb{R}^d$  and project their loss Hessian onto the nullspace of  $B \in \mathbb{R}^{d \times (t-1)k}$ . From the resulting projection, we append the top  $k$  eigenvectors to  $B$ . We compute the eigenvectors using Hessian-vector products [11] to avoid explicitly constructing the full Hessian matrix. The resulting basis is designed to include directions of highest curvature at each checkpoint so that it will capture synchronized loss behavior throughout training. Note that the very top eigenvectors are likely to reflect local oscillation, rather than conceptually meaningful long-term movement [31], but as we continue to add to the low rank basis, we include more directions of long-term stable movement. We discard the oscillatory directions which do not provide an overall decrease in loss over the course of training according to POLCA.

### 3.2 Decomposing the loss with Projection Oriented Loss Change Allocation (POLCA)

To decompose the loss along our basis, we propose a modified version of Loss Change Allocation (LCA) [15]. LCA is a tool for analyzing changes in aggregated loss on dataset  $X$  between two checkpoints. The output of LCA is the empirical loss change between a pair of checkpoints which can be attributed to the motion of each individual weight unit. Given two consecutive checkpoints with parameters  $\theta_t$  and  $\theta_{t+1}$ , LCA reformulates the change in loss as its first-order Taylor approximation, a sum of the loss changes attributed to the movement of each individual model parameter  $\theta^{(j)}$ :

$$L(X; \theta_{t+1}) - L(X; \theta_t) \approx \sum_{j=0}^d (\nabla_{\theta} L(X; \theta_t))^{(j)} (\theta_{t+1}^{(j)} - \theta_t^{(j)}) \quad (1)$$

$$= \sum_{j=0}^d LCA(X; \theta^{(j)}) \quad (2)$$

The POLCA decomposition differs from LCA in three key ways. First, we do not restrict each direction to correspond to a single unit  $\theta^{(j)}$ , instead permitting an *arbitrary* orthonormal basis vector  $b \in B$  to replace the axis-aligned basis vectors in LCA; we project onto this basis vector using the dot product  $\langle b, \cdot \rangle$ . Second, we are interested in changes in the loss on each individual example  $x \in X$ , not the entire dataset  $X$ . These first two modifications provide the following reformulation of LCA.

$$L(X; \theta_{t+1}) - L(X; \theta_t) = \sum_{x \in X} L(x; \theta_{t+1}) - L(x; \theta_t) \quad (3)$$

$$\approx \sum_{x \in X} \sum_{b \in B} \langle b, \nabla_{\theta} L(x; \theta_t) \rangle \langle b, \theta_{t+1} - \theta_t \rangle \quad (4)$$

The third key difference is that we must use a second-order approximation because this basis is constructed explicitly from the Hessian eigenvectors. To understand why this choice of basis requires a second-order approximation, recall that each basis vector  $b$  is an eigenvector of the Hessian matrix  $\mathcal{H}_{t'}(X)$  at some timestep  $t'$ , where  $b$  is chosen because it has the largest eigenvalue  $\lambda_{t'}(X, b)$  over

the whole dataset. If we assume that the top eigenvectors of the aggregate Hessian maintain high curvature at other points in training and on individual datapoints, then the scaling factor in the second-order Taylor term will be very large even at the datapoint level. Limiting the approximation to only the first order term gives poor guarantees on error, as the second-order term could be expected to dominate. We find that empirically, the difference between the first and second-order values is small (Appendix F), but compute the second-order approximation to guarantee a better estimate.

Exact computation of the second-order term would be intractable, requiring computation of the top eigenvalues/vectors for each individual datapoint  $x$ . Instead, we can approximate it by substituting the true eigenvalue, denoted  $\lambda_t(X, b) := b^\top \mathcal{H}_t(X)b$ , with the curvature of the individual loss in the direction  $b$ , i.e.  $\lambda_t(x, b) = b^\top \mathcal{H}_t(x)b$ . If the aggregate Hessian eigenvector  $b$  is close to the span of the top eigenvectors of the datapoint-specific Hessian for  $x$ , this provides a reasonable estimate while reducing calculation to a single Hessian-vector product per eigenvector. We therefore approximate the basis projection of the datapoint Hessian  $h(x, b, \theta_t)$  as derived in Appendix A.

$$h(x, b, \theta_t) = \frac{\lambda_t(x, b)}{2} \langle \theta_{t+1} - \theta_t, b \rangle^2 \quad (5)$$

$$\approx \frac{\lambda_t(X, b)}{2} \cdot \langle \theta_{t+1} - \theta_t, b \rangle^2 \times \frac{\langle L(x; \theta_{t+1}) - L(x; \theta_t), b \rangle}{\langle L(X; \theta_{t+1}) - L(X; \theta_t), b \rangle} \quad (6)$$

$$= \tilde{h}(x, b, \theta_t) \quad (7)$$

Equipped with this second-order approximation of the datapoint Hessian’s projection onto our basis, we account for the high curvature and possible domination by the higher order term by modifying Equation 4 into the second-order Taylor expansion using the [approximation](#) from Equation 7.

$$L(X; \theta_{t+1}) - L(X; \theta_t) \approx \sum_{x \in X} \sum_{b \in B} \langle b, \nabla_\theta L(x; \theta_t) \rangle \langle b, \theta_{t+1} - \theta_t \rangle + \tilde{h}(x, b, \theta_t) \quad (8)$$

$$= \sum_{x \in X} \sum_{b \in B} \text{POLCA}(x, b; \theta_t) \quad (9)$$

### 3.3 Clustering the loss

POLCA, above, provides curves that show how a decomposed loss changes with respect to each training example. We assume that if several examples show similarly timed loss changes in the same direction, they likely rely on the same conceptual breakthroughs or learning events; therefore, they are likely to share a required skill. We cluster POLCA training histories to recover these skill groups. For each datapoint  $x$ , we compute the total cumulative change in loss along each basis vector  $b$  by summing over the previous POLCA values. We denote this sum the **projected loss**  $L_b(x, \theta_t)$ .

$$L_b(x, \theta_t) = \sum_{i=0}^{t-1} \text{POLCA}(x, b; \theta_i) \quad (10)$$

We obtain 1d projected loss trajectories for breakthrough clustering by computing  $L_b(x, \theta_t)$  at every time  $t$ . As our clustering algorithm, we choose Hierarchical Density-Based Spatial Clustering of Applications with Noise (HDBSCAN) [5] because it distinguishes cluster outliers and discovers clusters with variable density (i.e., similarly shaped curves that lay far apart in their metrics).

## 4 Arithmetic language modeling

We validate our POLCA clustering method in a synthetic setting using an arithmetic addition task. Our clusters reflect categorical concepts within the data, even when those concepts are not discoverable by clustering directly on loss curves. Specifically, if we cluster on exact loss curves we recover digit positions, but if we cluster on POLCA curves we also recover the skill of “carrying” a digit.

### 4.1 Experiments

**Data** Our synthetic experiments use data from the arithmetic addition setting in Chen et al. [7], where the model is trained to compute the sum of two 3-digit numbers. As shown in Appendix Figure

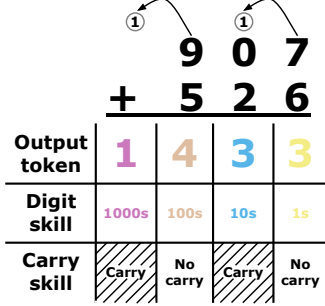


Figure 2: **Diagram of arithmetic addition task.** An example of 3-digit addition, labeled with the skills required for each of the output tokens.

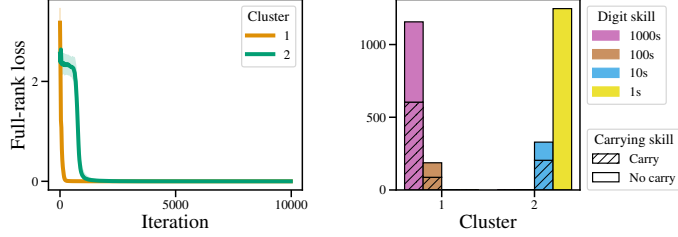


Figure 3: **Exact loss trajectory clustering on the arithmetic task.** We use HDBSCAN to cluster the exact loss trajectories. This approach, unlike our POLCA clustering method, fails to recover clusters associated with the carrying skill (the maximum fraction of carries is 0.514).

6 and Chen et al. [7], the skills corresponding to the digits have different loss curves, so we will easily recover the digit skill categories by clustering exact loss curves. Unlike our source material, we also consider an additional skill: arithmetic carries to the output token (Figure 2). Digit-specific addition skills lead to clearly distinguishable loss curves, whereas carrying skills are not clear from the exact loss (Appendix Figure 7), but become clear on the decomposed gradient basis.

**Setup details** We train a 3-layer (9m parameter) Transformer model with embedding dimension 512, 4 attention heads per layer, and an MLP dimension of 2048 [22]. We choose this model size to align with prior work Olsson et al. [24] and to maximize the granularity at which we can feasibly compute the POLCA values. For a validation set with 1250 data points and 5000 output tokens, we compute the loss and POLCA values for each token at intervals of 20 iterations throughout training. We choose the training steps between each POLCA computation to achieve as fine-grained analysis as possible without exploding the compute time. We compute the POLCA basis using the eigenvectors of the Hessian estimated using a 1250 data point sample of the training set as detailed in Algorithm 1. We compute one new basis vector every 200 iterations for a total of 50 basis vectors. We provide further ablations on the decomposition strategy and choice of POLCA basis in Appendix D and E.

**Clustering** To ensure that we are investigating directions where the model is learning on average, we only consider the basis vectors for which the mean projected loss decreases. Then for each remaining basis vector, we remove all of the tokens for which the decomposed loss increases. We use HDBSCAN to cluster the remaining tokens, discarding the tokens it marks as outliers. Through this process, we find subpopulations of the data that have similar projected loss trajectories.

## 4.2 Results

**Comparison to the exact loss** In our clustering experiments on arithmetic addition skills, we first consider whether directional decomposition is necessary for identifying individual concepts. As a baseline, we therefore cluster tokens solely on their exact loss curves for successive timesteps, rather than estimating the loss decomposed along a low rank basis.

According to the HDBSCAN loss clustering results in Figure 3, we can recover—to a substantial degree—the *digit* skill by clustering only on the exact loss, likely because the digits have very different loss trajectories. However, as shown in Figure 3 and Appendix Table 3, we cannot recover clusters that are homogenous with respect to the *carrying* from the exact loss alone.

**Recovering concepts with POLCA clustering** Because exact loss clustering failed to recover the carrying skill, we instead cluster on each basis vector’s projected loss using the POLCA decomposition. The projected loss value  $L_b(x, \theta_t)$  (Equation 10) represents the cumulative loss change of  $x$  attributed to movement along basis vector  $b$ . By clustering the projected loss trajectories, we find that the top 3 basis vectors produce homogeneous clusters corresponding to both digit and carrying skills for each of the digits (Figure 4 and Appendix Figure 8), so POLCA clustering is able to recover subtler skills, like carrying, that are challenging to reconstruct from the exact loss curves alone.

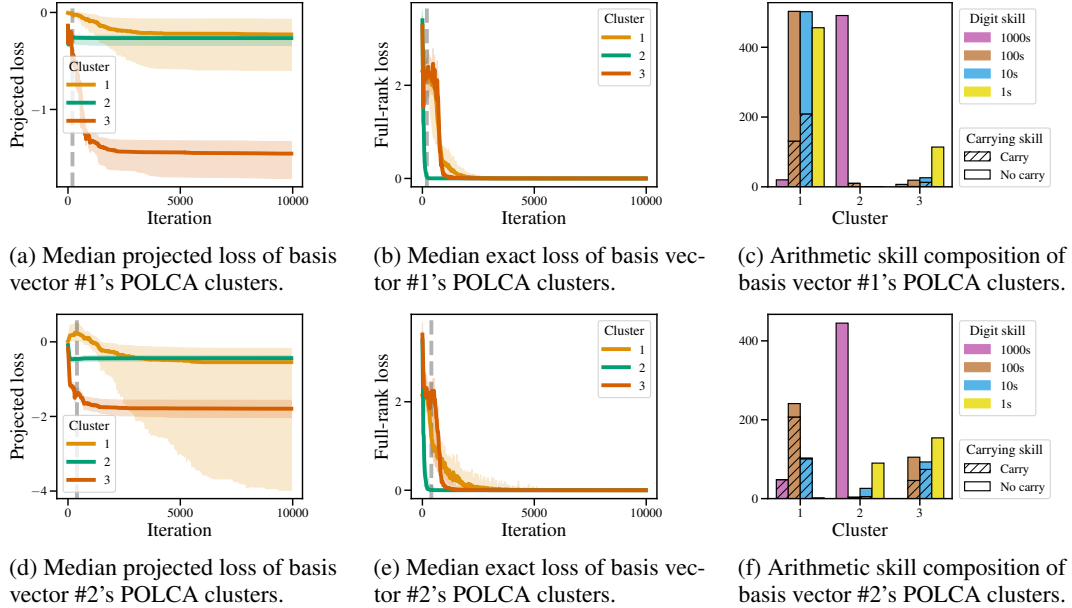


Figure 4: **Arithmetic data clusters with POLCA.** We perform POLCA clustering on the top 2 basis vectors, and report the cluster medoid and quartiles (*left*), median exact loss (*center*), and cluster skill composition (*right*) for each basis vector in order. Vertical lines mark the timestep when the relevant basis vector was sampled; note that a vector’s phase transitions are not directly associated with this timestep. We find that the first basis vector recovers the digit skill and cluster 1 of basis vector #2 recovers the carrying skill (with homogeneity 0.903). The clusters computed from the 1d projected loss POLCA trajectories show changes in the decomposed loss that are obscured in the exact loss curves.

Figure 4 shows the POLCA breakthrough clustering for the first three basis vectors. Along these directions, certain data subpopulations have changes in the projected loss (Figure 4a and 4d) that do not occur as visibly in their full loss curves (Figure 4b, 4e). *We conclude that arithmetic carries rely on breakthroughs along specific dimensions during training, but these breakthroughs may be elided in the exact loss curve.*

## 5 English language modeling

We apply our approach to a real-world causal language modeling task and show that POLCA breakthrough clustering recovers interpretable conceptual skills in the natural language setting.

### 5.1 Experiments

For the natural language modeling setting, we use the English Wikipedia dataset [35] from March 2022. We use the same POLCA setup as in the arithmetic addition setting. We train a 3-layer (40m parameter) transformer model with embedding dimension 512, 4 attention heads, and an MLP dimension of 2048 [22]. We compute the loss and POLCA values for each token on a validation set of 12600 output tokens. We analyze intermediate checkpoints at intervals of 200 iterations throughout training. We apply POLCA to the basis derived from the eigenvectors of the Hessian estimated using a 1000 data point sample of the training set as detailed in Algorithm 1 with  $k = 1$ . We compute a new basis vector every 750 iterations.

Similarly to the arithmetic setting, we only analyze the POLCA trajectories along the directions for which the decomposed loss decreases on average. We also discard any trajectories for which the decomposed per-token loss increases. After clustering the remaining token trajectories with HDBSCAN, we discard any marked as outliers before analysis.

## 5.2 Results

On language models, POLCA clustering again reveals hidden breakthroughs along each basis vector. To analyze the learned skills represented by each cluster, we look for syntactic and lexical patterns shared by the cluster data. After tagging tokens by part-of-speech (POS) using `spacy`, we label each cluster by computing its most common token and POS tag sequences. We confirm these automatically assigned cluster labels by examining the top 10 contexts closest to the medoid of the cluster.

We report a selection of clusters from specific basis vectors in Figure 5 (see Appendix H for more examples). Using POLCA clustering on projected loss trajectories for our basis vectors, we find token subpopulations that correspond to various grammatical constructions and have breakthroughs in the loss projected onto that basis. For instance, we show a cluster corresponding to predicting `< to>` and `< from>` after the first clause in a sentence in Figure 5a(ii). We also observe clusters whose projected loss trajectories move in opposing directions along certain basis vectors. For instance, in Figure 5b(i) and 5b(ii), cluster 1 contains appositive noun phrases and cluster 2 has noun phrases with similar syntactic patterns that are not appositive (such as list items). These clusters visibly mirror each other’s movement in direction, if not in magnitude—decreases in loss are generally larger than the opposing cluster’s increases in loss which mirror them.

Figure 5 shows that despite their smooth *exact* loss curves, POLCA clusters have sudden changes in their *decomposed* loss curves at different points during training. Clusters from the exact loss curves, by contrast, do not reveal breakthroughs except very early in training (Appendix Figure 9). We conclude that POLCA reveals breakthroughs in the decomposed loss that are obscured in the exact loss. Through clustering, POLCA can explain how different skills are learned during language model training.

## 6 Conclusions

This work introduces POLCA clustering, a method to identify learned skills from decomposed loss trajectories. POLCA decomposes the loss on two levels: individual datapoints and specific directions in the weight space. We use this decomposition to discover clusters that share breakthroughs obscured by loss metrics. In language modeling and synthetic settings, these clusters recover interpretable skills which appear to emerge at particular moments during training.

These are promising findings for meaningfully interpreting large models. By recovering breakthroughs in identifiable skills, we support the hypothesis that high-dimensional learning typically entails a series of phase transitions at various scales. When a phase transition appears in training, it suggests a naturally discrete category; the model either knows the concept or doesn’t know it, with little middle ground. Humans think in categorical concepts, so they are far more interpretable than the continuous data interpolations that appear in much of learning theory.

**Limitations** Our method of constructing a basis is inspired by the existing literature on training in restricted subspaces, but represents an obvious site of improvement. The top eigenvectors of the Hessian, like the axis-aligned basis, could represent many concepts in superposition. Therefore, some non-orthogonal basis might represent interpretable concepts more cleanly than our orthogonal basis, though it would no longer provide a low-rank decomposition. Furthermore, our basis is constructed by local curvature and then filtered to favor directions of long-term movement; other bases may favor long-term movement by construction. In general, we consider the ideal basis to be an open question.

We use small models so that we can have very fine-grained checkpoints for POLCA computation. Scaling this work to larger models may require using a basis that is less computationally expensive to compute than Hessian eigenvectors, but our results from Appendix E indicate that this is likely possible with limited impact on the cluster quality.

## Acknowledgements

This work was informed by helpful conversations with Nikhil Vyas, Nicholas Lourie, Mike Lepori, and Ekdeep Singh Lubana. This material is based upon work supported by the National Science Foundation Graduate Research Fellowship under Grant No. DGE 2140743. Any opinion, findings, and conclusions or recommendations expressed in this material are those of the authors(s) and do not

necessarily reflect the views of the National Science Foundation. This work was enabled in part by a gift from the Chan Zuckerberg Initiative Foundation to establish the Kempner Institute for the Study of Natural and Artificial Intelligence.

## References

- [1] E. Abbe, E. Boix-Adsera, M. Brennan, G. Bresler, and D. Nagaraj. The staircase property: How hierarchical structure can guide deep learning, 2021.
- [2] A. Achille, M. Rovere, and S. Soatto. Critical learning periods in deep neural networks. *CoRR*, abs/1711.08856, 2017. URL <http://arxiv.org/abs/1711.08856>.
- [3] S. Arora and A. Goyal. A theory for emergence of complex skills in language models. *arXiv preprint arXiv:2307.15936*, 2023.
- [4] A. Bhaskar, D. Friedman, and D. Chen. The Heuristic Core: Understanding Subnetwork Generalization in Pretrained Language Models, June 2024. URL <http://arxiv.org/abs/2403.03942>. arXiv:2403.03942 [cs].
- [5] R. J. G. B. Campello, D. Moulavi, and J. Sander. Density-based clustering based on hierarchical density estimates. In J. Pei, V. S. Tseng, L. Cao, H. Motoda, and G. Xu, editors, *Advances in Knowledge Discovery and Data Mining*, pages 160–172, Berlin, Heidelberg, 2013. Springer Berlin Heidelberg. ISBN 978-3-642-37456-2.
- [6] A. Chen, R. Shwartz-Ziv, K. Cho, M. L. Leavitt, and N. Saphra. Sudden drops in the loss: Syntax acquisition, phase transitions, and simplicity bias in mlms, 2024.
- [7] M. Chen, N. Roberts, K. Bhatia, J. Wang, C. Zhang, F. Sala, and C. Ré. Skill-it! a data-driven skills framework for understanding and training language models. *Advances in Neural Information Processing Systems*, 36, 2024.
- [8] J. M. Cohen, S. Kaur, Y. Li, J. Z. Kolter, and A. Talwalkar. Gradient descent on neural networks typically occurs at the edge of stability, 2022.
- [9] F. Draxler, K. Veschgini, M. Salmhofer, and F. A. Hamprecht. Essentially No Barriers in Neural Network Energy Landscape. *arXiv:1803.00885 [cs, stat]*, Feb. 2019. URL <http://arxiv.org/abs/1803.00885>. arXiv: 1803.00885.
- [10] J. Frankle, G. K. Dziugaite, D. Roy, and M. Carbin. Linear mode connectivity and the lottery ticket hypothesis. In *International Conference on Machine Learning*, pages 3259–3269. PMLR, 2020.
- [11] N. Golmant, Z. Yao, A. G. Gholami, M. Mahoney, and J. Gonzalez. pytorch-hessian-eigenthings: efficient pytorch hessian eigendecomposition, Oct. 2018. URL <https://github.com/noahgolmant/pytorch-hessian-eigenthings>.
- [12] G. Gur-Ari, D. A. Roberts, and E. Dyer. Gradient descent happens in a tiny subspace, 2018.
- [13] S. Jastrzębski, M. Szymczak, S. Fort, D. Arpit, J. Tabor, K. Cho\*, and K. Geras\*. The break-even point on optimization trajectories of deep neural networks. In *International Conference on Learning Representations*, 2020.
- [14] J. Juneja, R. Bansal, K. Cho, J. Sedoc, and N. Saphra. Linear connectivity reveals generalization strategies. In *The Eleventh International Conference on Learning Representations*, 2023. URL <https://openreview.net/forum?id=hY6M0JH13uL>.
- [15] J. Lan, R. Liu, H. Zhou, and J. Yosinski. Lca: Loss change allocation for neural network training, 2020.
- [16] C. Lovering, J. Forde, G. Konidaris, E. Pavlick, and M. Littman. Evaluation beyond task performance: Analyzing concepts in alphazero in hex. *Advances in Neural Information Processing Systems*, 35:25992–26006, 2022.
- [17] E. S. Lubana, E. J. Bigelow, R. P. Dick, D. Krueger, and H. Tanaka. Mechanistic mode connectivity, 2023. URL <https://arxiv.org/abs/2211.08422>.
- [18] C. Ma, D. Kunin, L. Wu, and L. Ying. Beyond the quadratic approximation: the multiscale structure of neural network loss landscapes. *arXiv preprint arXiv:2204.11326*, 2022.

- [19] T. McGrath, A. Kapishnikov, N. Tomašev, A. Pearce, M. Wattenberg, D. Hassabis, B. Kim, U. Paquet, and V. Kramnik. Acquisition of chess knowledge in alphazero. *Proceedings of the National Academy of Sciences*, 119(47):e2206625119, 2022.
- [20] E. J. Michaud, Z. Liu, U. Girit, and M. Tegmark. The quantization model of neural scaling, 2024.
- [21] S. Murty, P. Sharma, J. Andreas, and C. D. Manning. Grokking of hierarchical structure in vanilla transformers. *arXiv preprint arXiv:2305.18741*, 2023.
- [22] N. Nanda and J. Bloom. Transformerlens. <https://github.com/TransformerLensOrg/TransformerLens>, 2022.
- [23] N. Nanda, L. Chan, T. Lieberum, J. Smith, and J. Steinhardt. Progress measures for grokking via mechanistic interpretability, 2023. URL <https://arxiv.org/abs/2301.05217>.
- [24] C. Olsson, N. Elhage, N. Nanda, N. Joseph, N. DasSarma, T. Henighan, B. Mann, A. Askell, Y. Bai, A. Chen, T. Conerly, D. Drain, D. Ganguli, Z. Hatfield-Dodds, D. Hernandez, S. Johnston, A. Jones, J. Kernion, L. Lovitt, K. Ndousse, D. Amodei, T. Brown, J. Clark, J. Kaplan, S. McCandlish, and C. Olah. In-context learning and induction heads, 2022. URL <https://arxiv.org/abs/2209.11895>.
- [25] C. Olsson, N. Elhage, N. Nanda, N. Joseph, N. DasSarma, T. Henighan, B. Mann, A. Askell, Y. Bai, A. Chen, et al. In-context learning and induction heads. *arXiv preprint arXiv:2209.11895*, 2022.
- [26] A. Potapczynski, M. Finzi, G. Pleiss, and A. G. Wilson. CoLA: Exploiting Compositional Structure for Automatic and Efficient Numerical Linear Algebra. *arXiv preprint arXiv:2309.03060*, 2023.
- [27] A. Power, Y. Burda, H. Edwards, I. Babuschkin, and V. Misra. Grokking: Generalization beyond overfitting on small algorithmic datasets. *arXiv preprint arXiv:2201.02177*, 2022.
- [28] T. Qin, N. Saphra, and D. Alvarez-Melis. Sometimes i am a tree: Data drives unstable hierarchical generalization, 2024. URL <https://arxiv.org/abs/2412.04619>.
- [29] E. Rosenfeld and A. Risteski. Outliers with opposing signals have an outsized effect on neural network optimization. In *The Twelfth International Conference on Learning Representations*, 2024.
- [30] R. Shwartz-Ziv and N. Tishby. Opening the black box of deep neural networks via information, 2017. URL <https://arxiv.org/abs/1703.00810>.
- [31] M. Song, K. Ahn, and C. Yun. Does SGD really happen in tiny subspaces? In *High-dimensional Learning Dynamics 2024: The Emergence of Structure and Reasoning*, 2024. URL <https://openreview.net/forum?id=iITzMuv9sL>.
- [32] G. Wang, J. Hoogland, S. van Wingerden, Z. Furman, and D. Murfet. Differentiation and specialization of attention heads via the refined local learning coefficient. *ArXiv*, abs/2410.02984, 2024. URL <https://api.semanticscholar.org/CorpusID:273162605>.
- [33] S. Watanabe. Asymptotic equivalence of bayes cross validation and widely applicable information criterion in singular learning theory. *ArXiv*, abs/1004.2316, 2010. URL <https://api.semanticscholar.org/CorpusID:15093314>.
- [34] S. Wei, D. Murfet, M. Gong, H. Li, J. Gell-Redman, and T. Quella. Deep learning is singular, and that’s good. *IEEE Transactions on Neural Networks and Learning Systems*, 34:10473–10486, 2020. URL <https://api.semanticscholar.org/CorpusID:225041126>.
- [35] Wikimedia Foundation. Wikimedia downloads, 2022. URL <https://dumps.wikimedia.org>.
- [36] M. Xia, M. Artetxe, C. Zhou, X. V. Lin, R. Pasunuru, D. Chen, L. Zettlemoyer, and V. Stoyanov. Training trajectories of language models across scales, 2023.

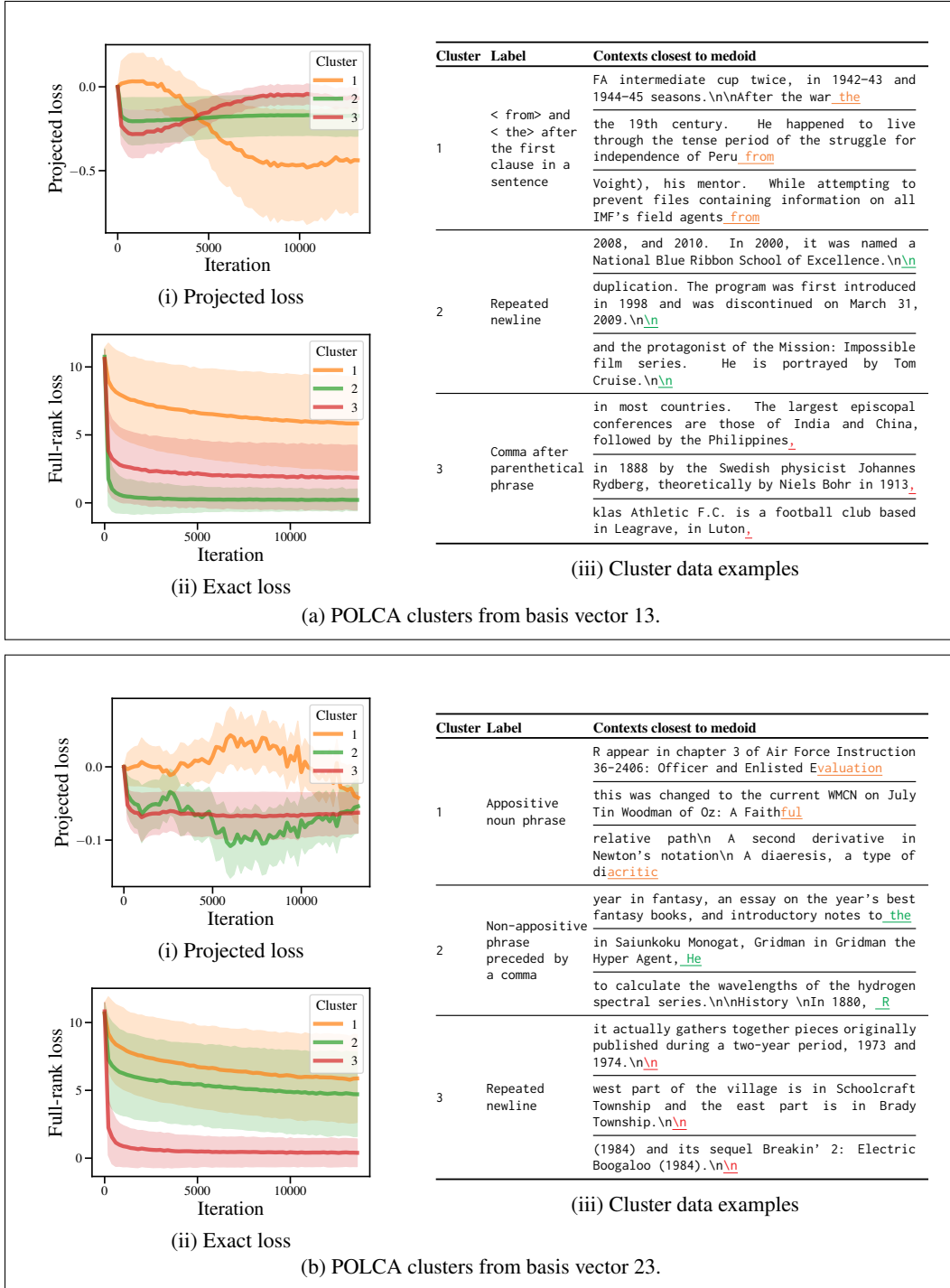


Figure 5: **Examples of English LM data clusters with POLCA.** After clustering on POLCA trajectories for two illustrative basis vectors, we report their average decomposed POLCA trajectories (5a(i) and 5b(i)). Figures 5a(ii) and 5b(ii) show the average of the exact loss trajectories for each of the POLCA trajectory clusters. For each cluster, we provide a label based on the top POS tags and tokens in the cluster and the top 10 contexts closest to its medoid. We report the 3 contexts closest to the cluster medoid and color the corresponding token. Clustering on the decomposed POLCA trajectories reveals low-rank breakthroughs at times when the full-rank exact loss curve remains smooth.

## A Derivation of approximate second-order term

We can approximate the difference between the gradient at time  $t$  and  $t + 1$  as

$$g_{t+1}(X) - g_t(X) \approx \mathcal{H}_t(X)(\theta_{t+1} - \theta_t) \quad (11)$$

$$\langle g_{t+1}(X) - g_t(X), b \rangle \approx b^\top \mathcal{H}_t(X) b \langle b, \theta_{t+1} - \theta_t \rangle \quad (12)$$

$$= \lambda_t(X) \langle b, \theta_{t+1} - \theta_t \rangle \quad (13)$$

If we assume  $b$  to also be an eigenvector of the datapoint Hessians  $\mathcal{H}'_t(x)$ , we can apply a similar argument for the gradient on the datapoint level.

$$\langle g'_{t+1}(x) - g'_t(x), b \rangle \approx b^\top \mathcal{H}'_t(x) b \langle b, \theta_{t+1} - \theta_t \rangle \quad (14)$$

Note that the assumption above (of matching Hessian eigenvectors between data points and their aggregate) is unlikely to be correct. If this assumption is violated, then the scaling factor in the following second-order Taylor term will be minuscule on the datapoint level. In practice, we have found that the second-order term has limited impact at the datapoint level (see Appendix F), but we nonetheless use it to improve our approximation. Then we may approximate it as:

$$\frac{\langle g'_{t+1}(x) - g'_t(x), b \rangle}{\langle g_{t+1}(X) - g_t(X), b \rangle} \approx \frac{b^\top \mathcal{H}'_t(x) b \langle b, \theta_{t+1} - \theta_t \rangle}{\lambda_t(X, b) \langle b, \theta_{t+1} - \theta_t \rangle} \quad (15)$$

$$\frac{\langle g'_{t+1}(x) - g'_t(x), b \rangle}{\langle g_{t+1}(X) - g_t(X), b \rangle} \approx \frac{\langle h'_t(x), b \rangle \langle b, \theta_{t+1} - \theta_t \rangle}{\lambda_t(X, b) \langle b, \theta_{t+1} - \theta_t \rangle} \quad (16)$$

$$\lambda_t(X, b) \frac{\langle g'_{t+1}(x) - g'_t(x), b \rangle}{\langle g_{t+1}(X) - g_t(X), b \rangle} \approx \langle h'_t(x), b \rangle \quad (17)$$

## B Hyperparameters

In the tables below, we provide the hyperparameters used during training of the models in the synthetic arithmetic and language modeling settings. We use NVIDIA H100 80GB HBM3 GPUs for our experiments and run each training run on a single GPU.

Table 1: Hyperparameters for training the synthetic arithmetic model

HYPERPARAMETER	VALUE
Number of Parameters	9475594
Iterations	10000
Epochs	1
Batch size	64
Number of training tokens	2560000
Optimizer	AdamW
Learning rate	1e-5
Weight decay	0.1
Betas	(0.9, 0.95)
LR Schedule	$\min(i/100, 1.0)$

Table 2: Hyperparameters for training the natural language model

HYPERPARAMETER	VALUE
Number of Parameters	40274737
Iterations	14000
Epochs	1
Batch size	64
Number of training tokens	114688000
Optimizer	AdamW
Learning rate	1e-5
Weight decay	0.1
Betas	(0.9, 0.95)
LR Schedule	$\min(i/100, 1.0)$

### C Exact loss trajectories for the digit and carry skills

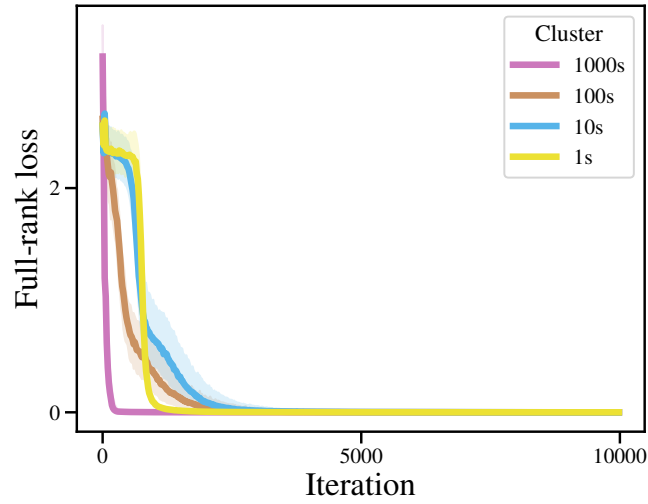


Figure 6: Median and quartiles of the loss trajectories for each digit.

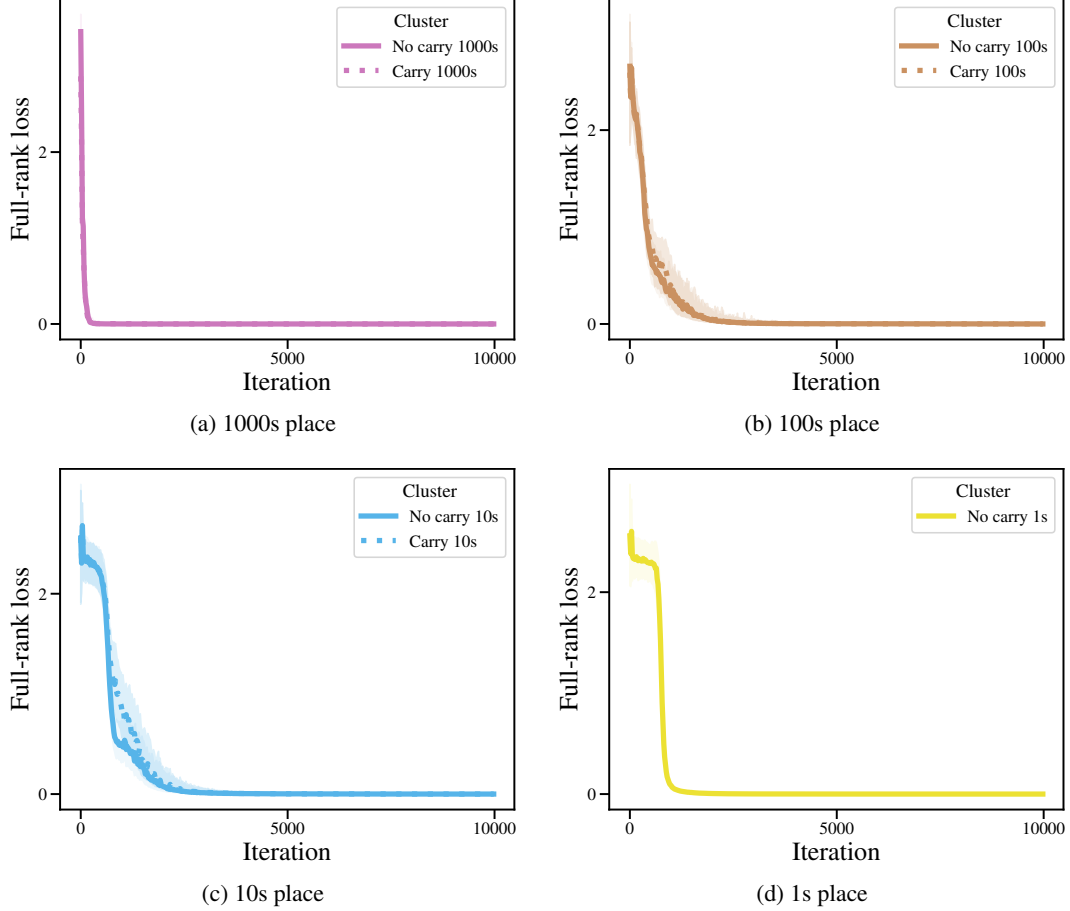


Figure 7: Median and quartiles of the loss trajectories for each digit and carry combination.

## D Decomposition strategy comparison

We investigate whether POLCA is required for decomposing the loss. We test three strategies:

- **Loss:** Exact loss
- **Fisher information:** We approximate the empirical Fisher Information as  $\|\nabla_{\theta} L(x, \theta_t)\|_2^2$  as in [2]. For each basis vector  $b$ , the Fisher Information projected onto  $b$  is  $\langle b, \nabla_{\theta} L(x, \theta_t) \rangle^2$ .
- **POLCA:** We compute the projected loss (Equation 9).

While using the projected gradient is less computationally intensive than computing the entire POLCA term, the results from Table 3 demonstrate that clustering on solely the Fisher information does not yield sufficiently homogeneous carry clusters.

Table 3: Carry skill homogeneity comparison. For each type of trajectory, we compute the fraction of points within each cluster that contain a carry to the output token and report the three maximum homogeneities across all 50 vectors. POLCA recovers three homogeneous carry clusters, while per-token loss and empirical Fisher information do not find any homogeneous carry clusters.

Decomposition strategy	Top vector skill homogeneities		
	1	2	3
Loss	0.514	-	
Fisher information	0.664	0.643	0.637
POLCA	0.973	0.946	0.903

## E POLCA basis comparison

We test ablated bases to analyze the effect of basis choice on the POLCA breakthrough clustering. To do so, we compute the maximum carry skill homogeneities over all of the clusters when performing POLCA breakthrough clustering. We use the following bases:

- **Random orthonormal:** randomly sampled orthonormal vectors
- **Random shuffled Hessian:** basis computed using Algorithm 1, but randomly shuffling the model checkpoints
- **Top Hessian eigenvectors:** basis computed using Algorithm 1

We find in Table 4 that these ablations result in only slightly less homogeneous carry clusters, indicating that different bases can be used for larger experiments to trade off between compute and interpretability.

Table 4: Carry skill homogeneity comparison. For each basis, we compute the fraction of points within each cluster that contains a carry to the output token and report the maximum homogeneities. Using the top Hessian eigenvectors recovers slightly more homogeneous carry clusters than the other basis selection strategies.

POLCA basis	Top vector skill homogeneities		
	1	2	3
Random orthonormal	0.902	0.858	0.838
Random shuffled Hessian	0.856	0.852	0.834
Top Hessian eigenvectors	0.973	0.946	0.903

## F Second versus first order POLCA approximation

Table 5: Empirical comparison of second and first order POLCA values. For the arithmetic setting, we compute the average cosine similarity and L2 distance between the second (Eq 9) and first (Eq 4) order POLCA trajectory vectors. The first and second-order approximations of the POLCA trajectories are very similar on average.

Cosine similarity	L2 norm
5.4891 E-4	0.99987

## G Additional arithmetic language modeling clusters

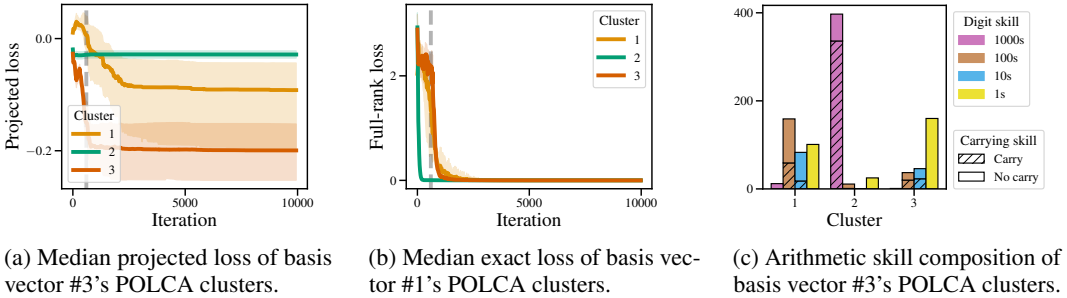


Figure 8: **Arithmetic data clusters with POLCA.** We perform POLCA clustering on the third basis vector, and report the cluster medoid and quartiles (*left*), median exact loss (*center*), and cluster skill composition (*right*). Vertical lines mark the timestep when the relevant basis vector was sampled; note that a vector's phase transitions are not directly associated with this timestep. We find that the third basis vector recovers the carrying skill in the 1000s place.

## H Additional natural language clusters

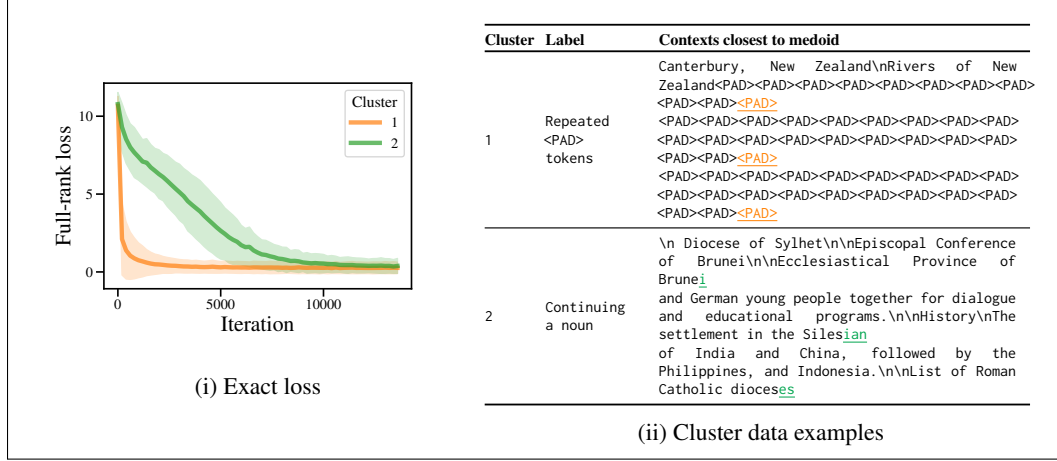


Figure 9: **English language modeling data clusters with the exact loss.** We cluster the exact loss trajectories and report the average loss by cluster (9i). For each cluster, we provide a label based on the top POS tags of tokens in the cluster and the top 10 contexts closest to the cluster medoid. We report the 3 contexts closest to the cluster medoid. Clustering on the loss trajectories only discovers a relatively simple skill, continuing nouns composed of multiple tokens. POLCA breakthrough clustering recovers a similar skill in Figures 10i and 10ii as well as discovering other skills.

